ACIPET

New model for prediction of corrected relative permeability by adjusting the prediction of poral throat radius incorporating static and dynamic tomography

Autor(es): ATarazona-R, A Bejarano-W, H Olaya, EIP, Universidad industrial de Santander; E Pérez-C, ECOPETROL S.A. Acipet,

Categoría: Marque con una “X”

• Artículo Técnico	X
• Tesis Pregrado	
• Tesis Posgrado	

ABSTRACT

Traditional estimation methods of flow units (J Leverett, Amaefule and Winland), tend to overestimate the pore throat radius, as in these equations effective porosity is in the denominator, mainly with the presence of low effective porosities (<10%), since normally low porosities are associated with low permeabilities and for these cases these methods tend to calculate high pore throat radius if effective porosity is used instead of total porosity.

The methodology proposed in this paper uses the poral throat radius and its distribution, estimates of capillary pressure, and calculations of relative permeabilities. With this methodology, effective porosity is generated from static tomography data and the other petrophysical variables (absolute permeability, relative permeabilities and saturation) are estimated and compared with core, logs and dynamic tomography results. A maximum pore throat radius is obtained from effective porosity and permeability. The capillary pressure, pore geometry and its saturation-related distribution are calculated.

This methodology was applied to the Mugrosa Formation in the Middle Magdalena Valley. The relative permeabilities obtained from the static tomography show that the Sor and Krw calculations should be improved in comparison with the results of the dynamic laboratory tomography performed on 'composites' of plugs.

Although good results are obtained for petrophysical variables using the proposed methodology, it is advisable to continue with the research of equations and / or numerical methods to model in a more exact way the phenomena of fluid displacement in the porous medium aimed at an effective integration of static tests with dynamic tests.

Keywords: permeability, microporosity, poral throat radius, capillary pressure, relative permeability

Resumen

Los métodos tradicionales de estimación de las unidades de flujo (J Leverett, Amaefule y Winland) tienden a sobreestimar el radio de la garganta de los poros, ya que en estas ecuaciones la porosidad efectiva está en el denominador, principalmente en presencia de bajas porosidades (<10%), ya que normalmente a bajas porosidades efectivas están asociadas bajas permeabilidades y para estos casos estos métodos tienden a calcular altos radios de la garganta de los poros si se usa la porosidad efectiva en vez de la porosidad total.

La metodología propuesta en este artículo utiliza el radio de garganta poral y su distribución, para realizar estimaciones de presión capilar y cálculos de permeabilidades relativas. Con esta metodología, la porosidad efectiva se genera a partir de los datos de tomografía estática, y las otras variables petrofísicas (permeabilidad absoluta, permeabilidades relativas y saturación) se estiman y comparan con los resultados de la tomografía de núcleos, registros y tomografías dinámicas. Se obtiene un radio máximo de garganta de poros a partir de una porosidad y permeabilidad efectivas. Adicionalmente se calcula la presión capilar, la geometría de los poros y su distribución relacionada con la saturación.

Esta metodología se aplicó a la Formación Mugrosa en el Valle del Magdalena Medio. Las permeabilidades relativas obtenidas de la tomografía estática muestran que los cálculos del Sor y Krw deben mejorarse en comparación con los resultados de la tomografía dinámica de laboratorio realizada en 'composites' de tapones.

Si bien se obtienen buenos resultados para las variables petrofísicas utilizando la metodología propuesta, es recomendable continuar con la investigación de ecuaciones y/o métodos numéricos para modelar de una manera más exacta los fenómenos de desplazamiento de fluidos en el medio poroso, estableciendo ajustes y procedimientos encaminados a una integración efectiva de las pruebas de tomografía estáticas y dinámicas.

Palabras claves: permeabilidad, microporosidad, radio de garganta poral, presión capilar, permeabilidad relativa.

Introduction

An appropriate description of the reservoir is an important factor in its characterization, since the definition of storage capacity (porosity) and ease to allow the production and / or movement of fluids (permeability) depend on this characterization. Critical variables such as porosity, permeability and hydrocarbon saturation define the prospective volumes and allow examining the behavior of fluids in the porous medium and the quality of the reservoir in terms of production. The most complex variable is permeability and the derived variables considering scaling, the vector nature, and the impact of reservoir heterogeneity on the definition as it was presented in the first work in Tarazona [1]; in addition to other aspects related to the acquisition of direct samples from all the wells in a field, scaling, and logging costs, among others, which limit areal and volumetric aspects of reservoir visualization Zhao [2].

The geological quality of the rocks generates different particular features, both morphological and textural, and in mineralogy, even so Ortiz [3], can be grouped into rock units represented in facies. Similarly, rock units are related to hydraulic units not only with the geological facie but with petrophysical properties such as porosity, permeability, saturation, and capillary pressure. The hydraulic quality is specifically related to the pore geometry as, if the texture and mineralogy are good attributes, the pore throat radius can characterize the hydraulic area properly. The integration of the f porosity, permeability, saturation, and capillary pressure parameters in the hydraulic unit is given by the concept of average radius of the hydraulic unit (rmh), which considers the equivalence of the porous medium with the capillary tubes for understanding the mechanisms by which fluids move Amaefule [4].

Flow units are very important for estimating reserves because the poral system controls the rock-fluid relationship, as well as the fluid flow, the distribution, the initial and residual volumes of hydrocarbon in the reservoir Fu [5]. To predict the performance of the flow unit for this project, an appropriate correlation is selected that enables determining the petrophysical variables and their combination for the various sections at different depths of the reservoir wells, with an appropriate scale.

The method to estimate permeability correlations is based on the Poiseuille equation, which considers the porous medium as cylinders with different diameters, where most of the parameters involved in the equation, can be acquired from Mercury Injection Porosimeter (MIP) curves. These results are obtained from laboratory measurement of plugs. The methodology used proposes a model that integrates pore geometry with capillary pressure and the calculation of relative permeability.

With the development of technology, multiple options for characterization of the poral environment have been created, such as dynamic X-ray computed tomography (CT). This method consists in obtaining the saturation profile of fluids (water and oil) in real time during their movement (waterflooding) through the poral medium to generate relative permeability curves. This method is novel and

has great potential, being a tool that collects high resolution images in a non-destructive way, facilitating the possibility of adapting flow conditions. Static tomography can be obtained where density, porosity and natural fractures of the sample Colin [6] can be calculated. It is determined that the saturations estimated from dynamic tomography contain less than 3% error as compared to the material balance Ortiz [3]. In this work comparisons between logs, cores, and static and dynamic tomography measurements are established. The proposed algorithms are applied to data originating from static tomography.

Theoretical framework

In 1960, Thomeer [7] established that the pore geometry and its dimensioning can be described mathematically in terms of capillary pressure by establishing a theoretical solution. In this paper, based on Thomeer's theory, a methodology is proposed for estimating capillary pressure, pore geometry and its distribution with respect to saturation from effective porosity and permeability.

It should be noted that the definition of flow units or rock types is related to solutions of equations that relate different petrophysical variables according to Wu [8], that is, from combinations of porosity, permeability and irreducible water saturation. These definitions are critical for the static and dynamic modeling of the reservoir, which helps to simplify and improve the construction of these models.

The starting point of the proposed solution for prediction of relative permeabilities is the evaluation of the maximum radius of the poral throat, according to Clerke [9], as will be seen later, for the estimation of capillary pressures vs. water saturation derived from Thomeer's original proposal by Harris [10] and after relative permeabilities proposed by Brooks [11].

To carry out the application of the proposed methodology, relative permeabilities calculation from logs, cores, density from static tomography, were compared versus results of relative permeabilities from dynamic tomograph. Likewise, given the different resolution of the available data, mechanisms were established to facilitate their comparison. The data scaling was performed using logs, cores and static tomography data first. Finally, results of relative permeability calculations from static tomography data are compared with relative permeabilities obtained in the dynamic tomography laboratory and relative permeabilities run in the Laboratory using non-steady state methods in plugs of the same rock type (Rock Type 2). This document delves deeper in the methodology presented at the SPWLA event Tarazona [1], where the development of the equations for prediction of relative permeability from static and dynamic tomography data was presented, incorporating also prediction of the poral throat radius.

Status of the technique

Several authors have proposed empirical correlations to obtain solutions in the definition of flow units as follows:

$$J(SW) = \frac{PC}{\sigma * COS(\theta)} * (\frac{K}{\emptyset e})^{0.5} \quad (1)$$

Leverett [12]

$$RQI = 0.0314 * \left(\frac{K}{\emptyset e}\right)^{0.5} \; o \; RQI = FZI * \frac{\emptyset e}{1-\emptyset e} \quad (2)$$

Amaefule [4]

$$R35 = 10^{0.732+0.588*LOG\ K-0.864*LOG\ \emptyset e} \quad (3)$$

Kolodzie [13]

These approaches, among others in the literature, Bejarano [14], allow to establish attributes of the poral system for the visualization of flow units. A specific issue related to the equations shown above is the effective porosity considered in the denominator of the equations, because when the value of the effective porosity is very low, by numerical approximation it generates very high values of the equations J, RQI and R35, leading to misinterpretation of the poral environment. To prevent this occurrence, it is suggested to use the following equation mentioned by Bejarano [14].

$$\emptyset e = \emptyset t * (1 - SWi) \quad (4)$$

The irreducible water saturation (SWi) represents the water that does not move in the poral system. The moving fluids are water

and hydrocarbons in a transition zone or only hydrocarbons if this zone is exceeded, which is equivalent to the effective or interconnected porosity. On the other hand, if the rock is oil-wet, the SWi is equal to the microporosity present in the rock. In accordance with the above, the Amaefule equation is modified according to Bejarano [14] and the RQI and FZI terms obtained are:

$$RQI = 0.0314 * \left(\frac{K*(1-SWi)}{\emptyset t}\right)^{0.5} = \frac{(1-SWi)^2}{SWi} * \frac{\emptyset e}{1-\emptyset e} \quad (5)$$

$$FZI = \frac{1-SWi}{SWi} \quad (6)$$

Thus, with the modifications made, the possible error in the description of the porous medium is corrected when low effective porosity values are replaced. Equation 6 allows calculating SWi since the porosity is known from the static tomography performed on full diameter cores, where a density curve (RHOB) is obtained. If the SWi is known, the permeability can be calculated from equation (5), and it can be applied to well logs. This would be the subject of future research. In this study, the correlation between porosity and core permeability (see figure 2) was used as regards static tomography to estimate irreducible water saturation. Sor (Residual Oil Saturation) saturation is estimated using the Ratio Method.

Similarly, it is possible to estimate the maximum poral throat radius as a function of porosity and permeability according to Clerke [9] and the minimum poral throat radius, knowing the SWi and the capillary pressure of displacement of mercury (PD). Then, the use of the following equations is proposed Bejarano [14]:

$$\text{Log2}* RGPmx = \left(\frac{\log K + 1.544 - 7.27*\emptyset e}{1.206}\right) \quad (7)$$

$$PD = \left(\frac{107}{RGPmax}\right) \quad (8)$$

The geometric porous factor Fg and the capillary pressure of mercury PC are estimates from Harris [10] equations:

$$Fg = 0.4342*(\text{Ln}(\frac{(5.21*K^{0.1254})}{\emptyset e}))^2 \quad (9)$$

$$\text{Log}\frac{PC}{PD} = -\frac{Fg}{Ln(1-SW)} \quad (10)$$

With the previous solutions, there is Capillary Pressure vs. Water Saturation, which facilitates calculation of relative permeabilities considering the Brooks [11] equations as follows:

$$SWw=(SW-SWi) / (1 - SWi) \quad (11)$$

$$Krw = Max (10^{-6}, (SWw^{(2-3*\lambda)/-\lambda}) \quad (12)$$

$$SWo=(SW-SWi) / (SXO - Swi) \quad (13)$$

$$Kro = Max (10^{-6}, Min (1, (1-Swo)^2 *(1-Swo^{(2-\lambda)/-\lambda})) \quad (14)$$

The value of λ used in equations 12 and 14 is calculated from the relationship between the corrected capillary pressure of mercury at capillary pressure oil-water and the corresponding water saturation. This study integrates data from different sources such as well logs, core, static tomography Ortiz [3] and dynamic tomography Ortiz [15, 16] as well as some capillary pressure results. As shown in Figure 1, the research is aimed at the comparative analysis and integration of the mentioned data.

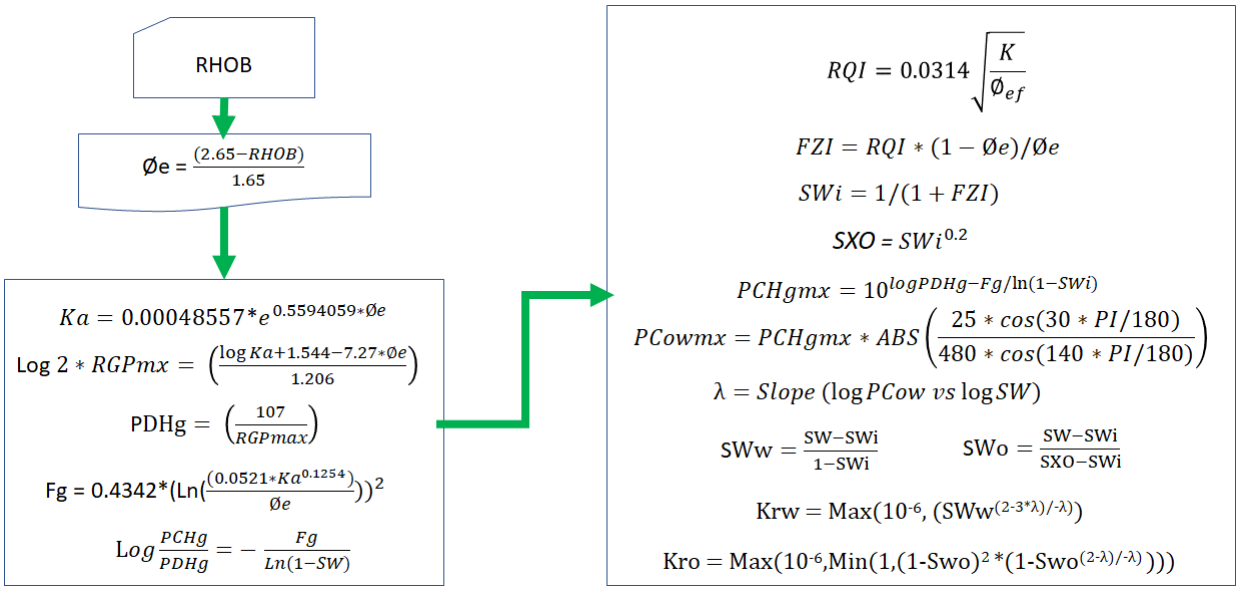

Figure 1.- Proposed Methodology Workflow. For the detail of the mathematical development of equations 1-14 used sequentially in the application of the methodology proposed in this work, the reader is suggested to consult the cited bibliographic references.

Experimental Development

The correlation for the permeability calculation was made from 77 available data sets (porosity vs air permeability) from plugs from cores between 5680.75 to 7307 feet (1626.25 feet) from the well VMM10. The correlation obtained is shown below:

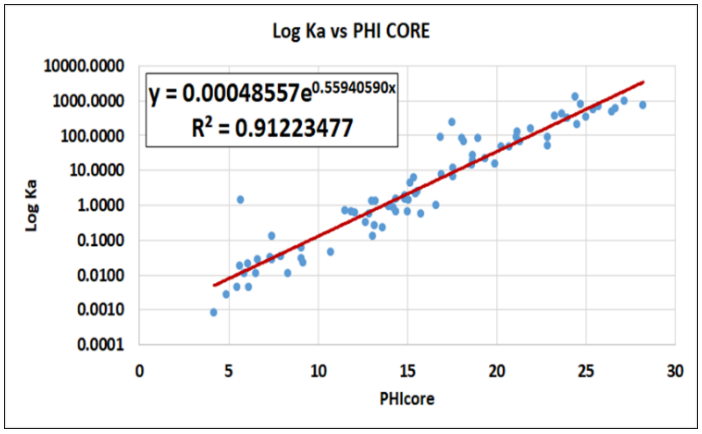

Figure 2.- Core Permeability vs Core Porosity correlation

RHOB density and PEF photoelectric potential are reported in the static tomography information. The porosity of static tomography is defined from the density published in laboratory analyses. The equation used is the same as that used in well logs when porosity is calculated from the density log. Due to the results of the XRD and SEM analysis, previously performed in the core analysis of the Mugrosa formation Pérez [17], sandstone lithology was taken by default and quartz density of 2.65 gr / cc and the water with a density of 1 gr / cc is used as fluid. The porosity used to calculate the relative permeabilities is equal to the effective porosity. However, it should be clarified that total porosity was initially obtained from static tomography and was converted to effective porosity using equation 4. Total available static tomography data are 74302 in the interval 5650.05-7313.44 feet (156.725 core feet) from the Well VMM10. In Table 1 the 5-core analyzed with tomography add up to 156.72 feet.

Core	Top (ft)	Base (ft)	h (ft)	Data (n)
C1	5.650,0472	5.652,8974	2.850	779
C2	5.680,0062	5.694,4668	14.461	6.702
C3	5.800,0082	5.857,0430	57.035	27.395
C4	6.364,0226	6.392,9767	28.954	13.530
C5	7.260,0185	7.313,4442	53.426	25.896
Total			156.725	74.302

Table 1.- Static tomography data

There are 474 static tomography data per foot, which require scaling to examine them with respect to the well logs data (spacing is 0.25 feet), that is, 4 data of one variable of logs per foot. It is observed that the vertical resolution of the obtained tomography is 118.5 times greater than that of logs. The estimated average values (633 data) were estimated from the quality control of the static tomography data using filters to eliminate empty data or with erroneous response of the core tomograph (Full Diameter Size), Table 2 examines the calculated percentiles of the static tomography.

Percentile	Depth	Density	PEF	Zeff	PHIDtom
fraction	ft	g/cc	barns/electron	barns/cc	fraction
0.00	5650.05	2.0501	1.2259	10.5822	**0.0010**
0.05	5686.43	2.1689	1.8955	11.9438	**0.0879**
0.10	5694.33	2.2293	1.9695	12.0716	**0.0994**
0.15	5807.53	2.2702	2.0240	12.1635	**0.1080**
0.20	5815.35	2.2963	2.0751	12.2480	**0.1161**
0.25	5823.10	2.3131	2.1197	12.3205	**0.1247**
0.30	5830.72	2.3274	2.1589	12.3835	**0.1334**
0.35	5838.30	2.3397	2.1990	12.4469	**0.1416**
0.40	5845.95	2.3513	2.2466	12.5213	**0.1495**
0.45	5853.58	2.3636	2.3099	12.6182	**0.1574**
0.50	6368.90	2.3767	2.3928	12.7424	**0.1656**
0.55	6376.59	2.3903	2.4836	12.8749	**0.1736**
0.60	6384.37	2.4034	2.5881	13.0232	**0.1810**
0.65	6392.75	2.4163	2.7089	13.1892	**0.1881**
0.70	7267.39	2.4299	2.8611	13.3910	**0.1955**
0.75	7274.96	2.4443	3.0110	13.5823	**0.2042**
0.80	7282.58	2.4584	3.1671	13.7744	**0.2144**
0.85	7290.16	2.4718	3.3306	13.9684	**0.2302**
0.90	7297.97	2.4860	3.5354	14.2018	**0.2550**
0.95	7305.55	2.5050	3.8479	14.5399	**0.2916**
1.00	7313.44	2.6497	13.9056	20.7756	**0.3636**

Table 2.-Percentiles of static tomography.

The estimated average values (633 data) vs. the original data (74302), in terms of porosity, are shown in Figure 3:

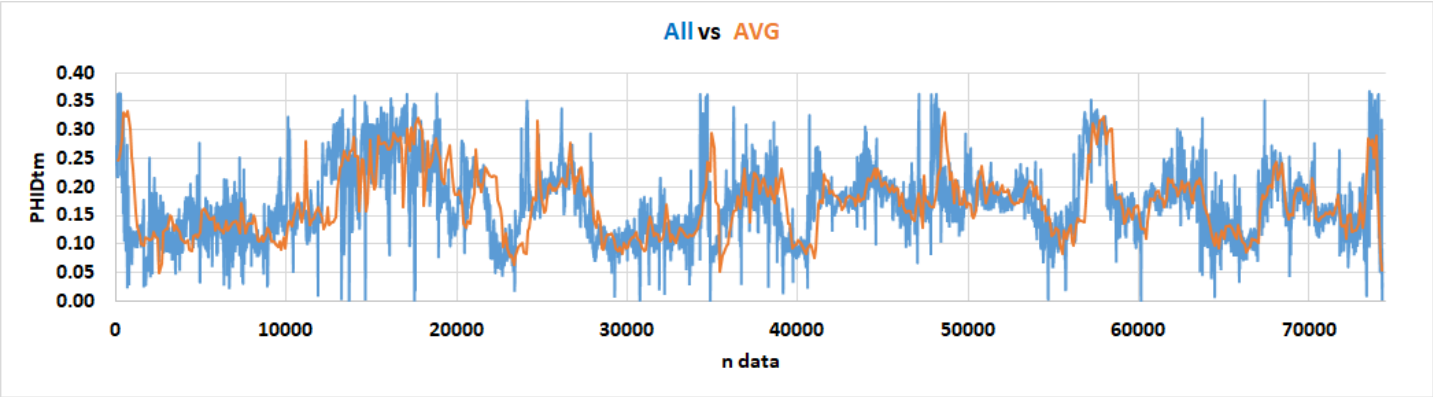

Figure 3.- Porosity of original and scaled tomography.

The differences are caused by reservoir heterogeneity. It should be noted that the PEF shows the presence of clays and materials other than sandstones, which should be the predominant lithology (PEF <2.5) in these deposits of continental origin (Figure 4). However, this PEF value <2.5, according to the criteria of the authors of this work, does not affect the porosity calculation from static tomography.

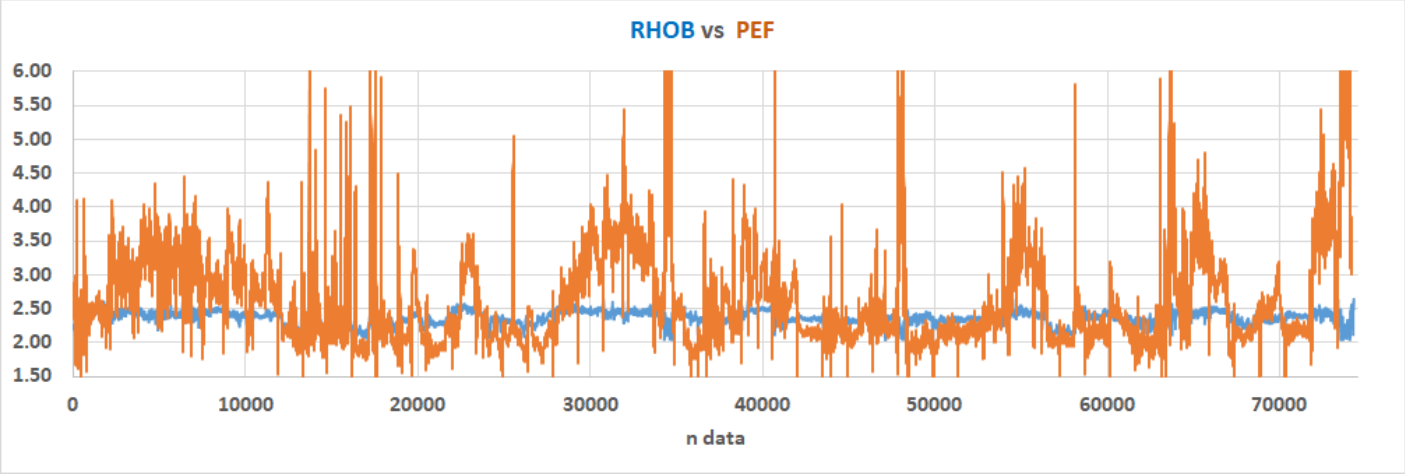

Figure 4.- Comparison between RHOB and PEF. On the X axis number of data and on the Y axis: PEF (barns /electron) and RHOB (gr / cc).

Results

For comparing well logs, cores and static tomography, the results of core 5 were used. Figure 5 shows the respective results. The impact of the hole quality is observed, visualized with the information quality index is right (ICI≤1), on the data from well logs as measurements are abnormal under these conditions (ICI> 1).

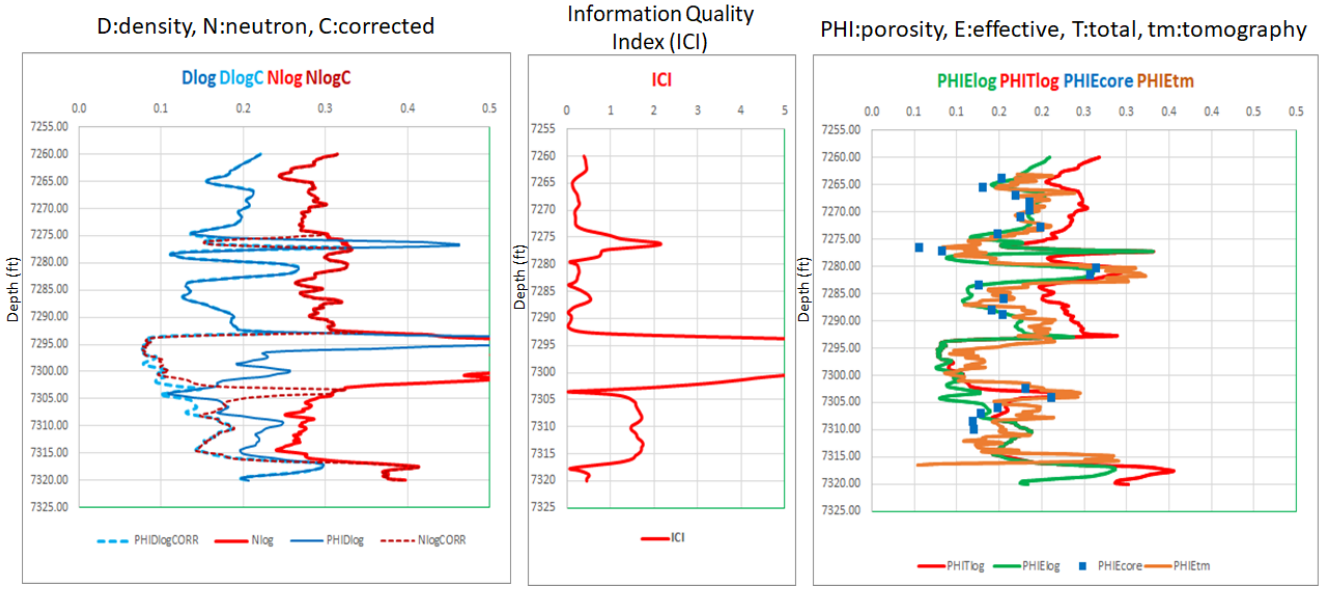

Figure 5.-Comparative logs, core and static tomography of the well VMM10.

Likewise, the static tomography measurements made on cores full diameter size correlate quite well with the RCAL plug data Pérez [17] and allow validating the corrected information in the logs. Based on the static tomography data using the proposed methodology (See figure 1), the displacement pressure PD of Clerke [9], the flow unit profile, and the irreducible water saturation present in core 5 are calculated. It is worth to highlight the correlation between PD and irreducible water saturation SWi.

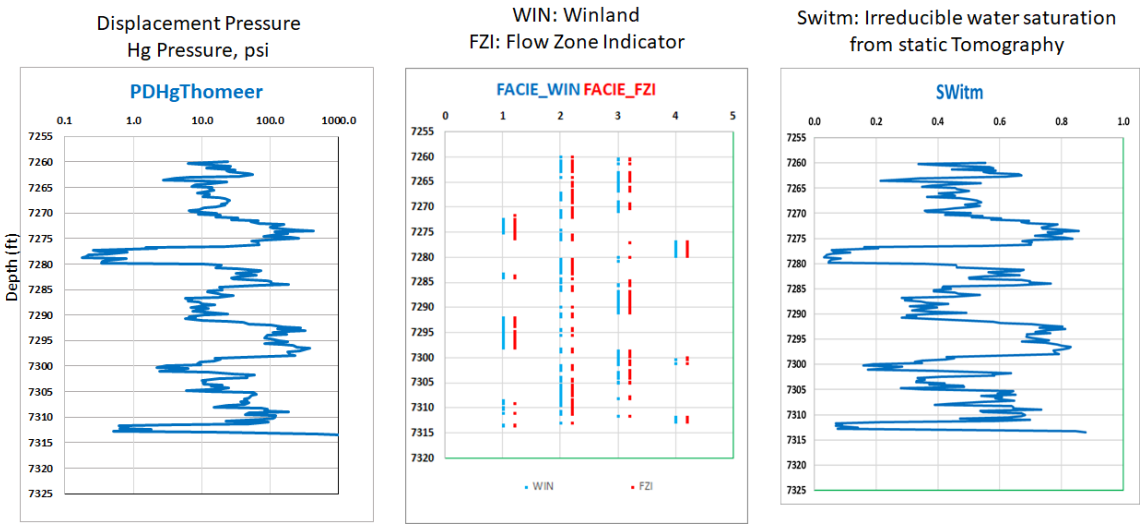

Figure 6.- Comparative of PD, Facies & SWi.

Figure 7 presents the calculated facies using the poral throat radius (PTR) cuts according to Winland. The data have been scaled and it shows pay and the product of facie value multiplied by pay in order to have a facie quality value.

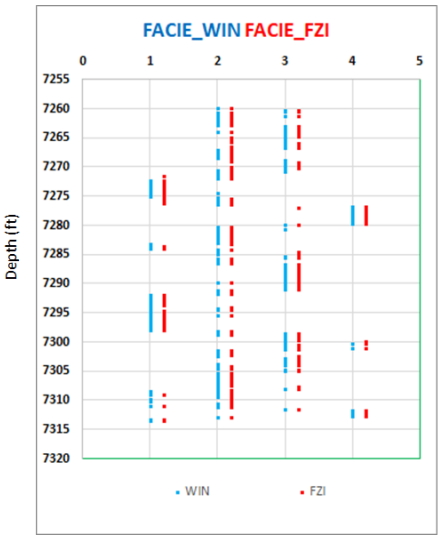

FACIE	WIN_H	WIN_VALUE	FZI_H	FZI_VALUE
1	11,00	11,00	10,75	10,75
2	21,25	42,50	22,50	45,00
3	16,25	48,75	15,25	45,75
4	5,00	20,00	5,00	20,00
Σ	53,50	122,25	53,50	121,50

VMM10 reference well

- The tomography information was reduced from 74302 to 633 data, calibrating the measurement to a depth similar to that of the logs.
- Due to the scale, it would be necessary to consider averages for the variables of interest.
- The permeability logarithm is practically linear vs porosity according to the core data in the VMM10 well.
- The average porosity will be arithmetic, and the average permeability will be geometric due to the core equation shown before.
- Flow units are defined using 4 facies calculations, Winland and FZI were used: the higher the value, the better the facies.

Figure 7.- Observations on facies.

Figure 8 shows the correlation of relative permeability estimates to water from static tomography (Figure 1) with the porosity data from logs, core and static tomography.

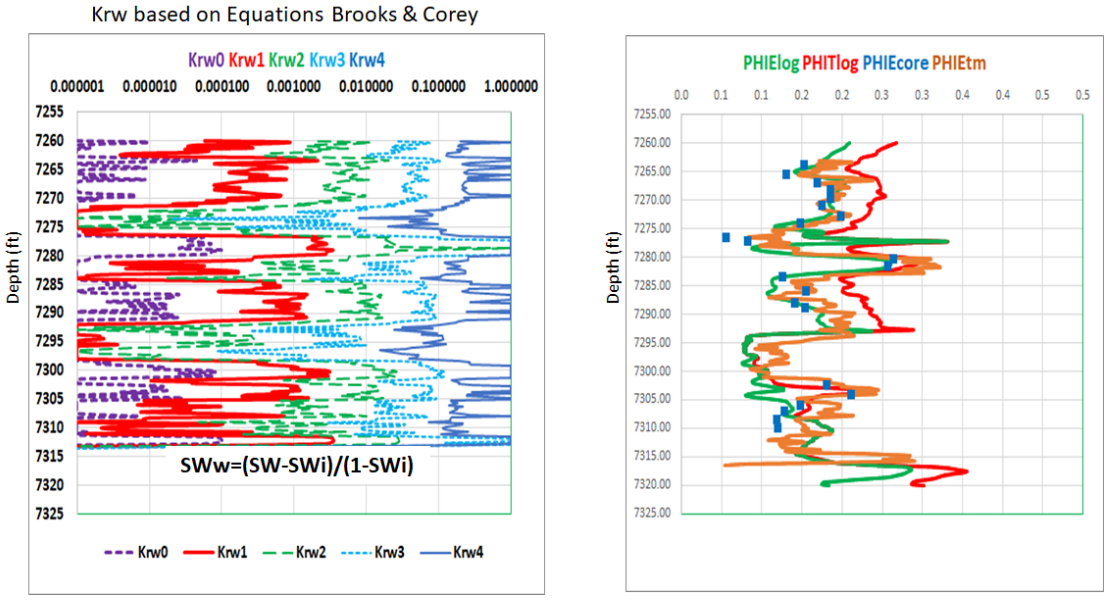

Figure 8.- Permeability relative to water vs. Porosities from logs, core and static tomography.

Figure 9 shows the petroleum relative permeability calculations for core 5 and the corresponding comparative with Logs, Cores and Static Tomography porosities.

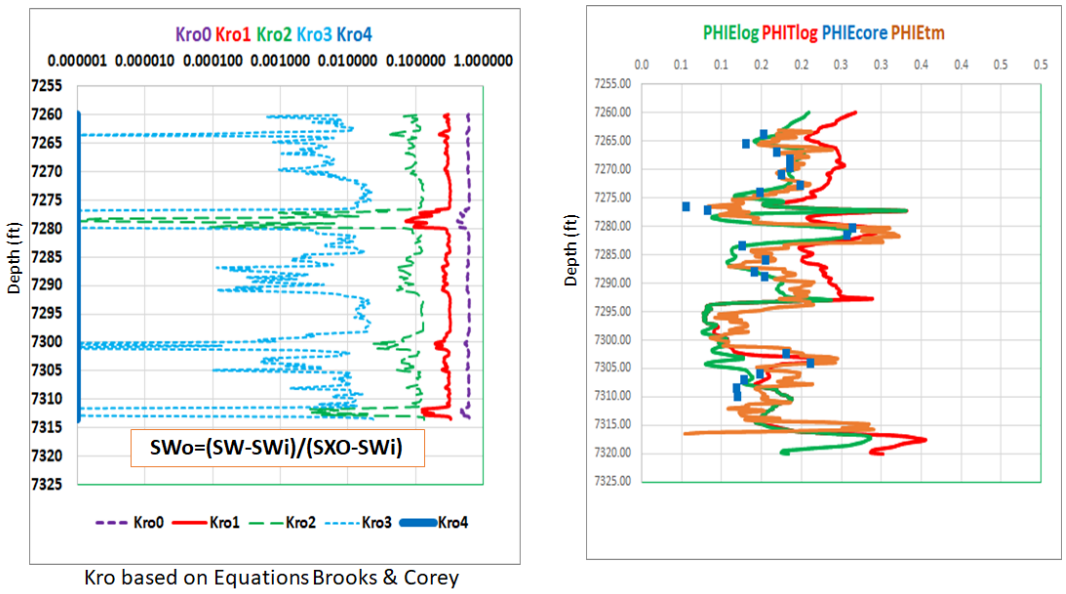

Figure 9.- Oil relative permeability vs Porosities from logs, cores and Static tomography.

Results in plugs

45 plugs from the Well VMM10 were examined. The results are shown in figure 10.

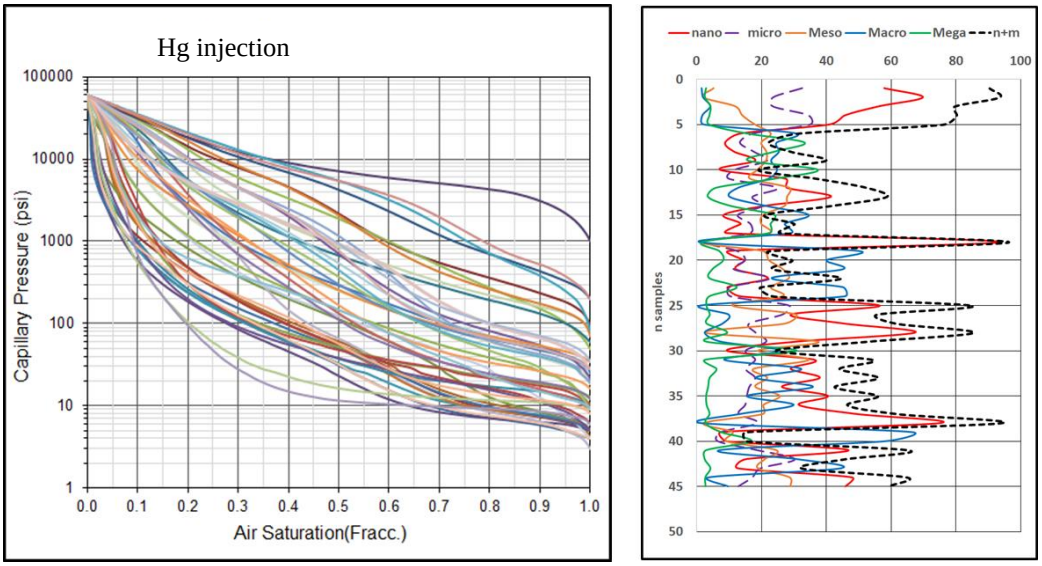

Figure 10.- Capillary pressures of 45 samples from the Well VMM10. In the graph on the right side: x-axis pore throat size in nanometers and Y-axis corresponds to the number of the sample ordered by increasing depth.

The heterogeneity of these samples should be noted according to the laboratory estimated poral throat size. There is abundant presence of nano plus microporosity.

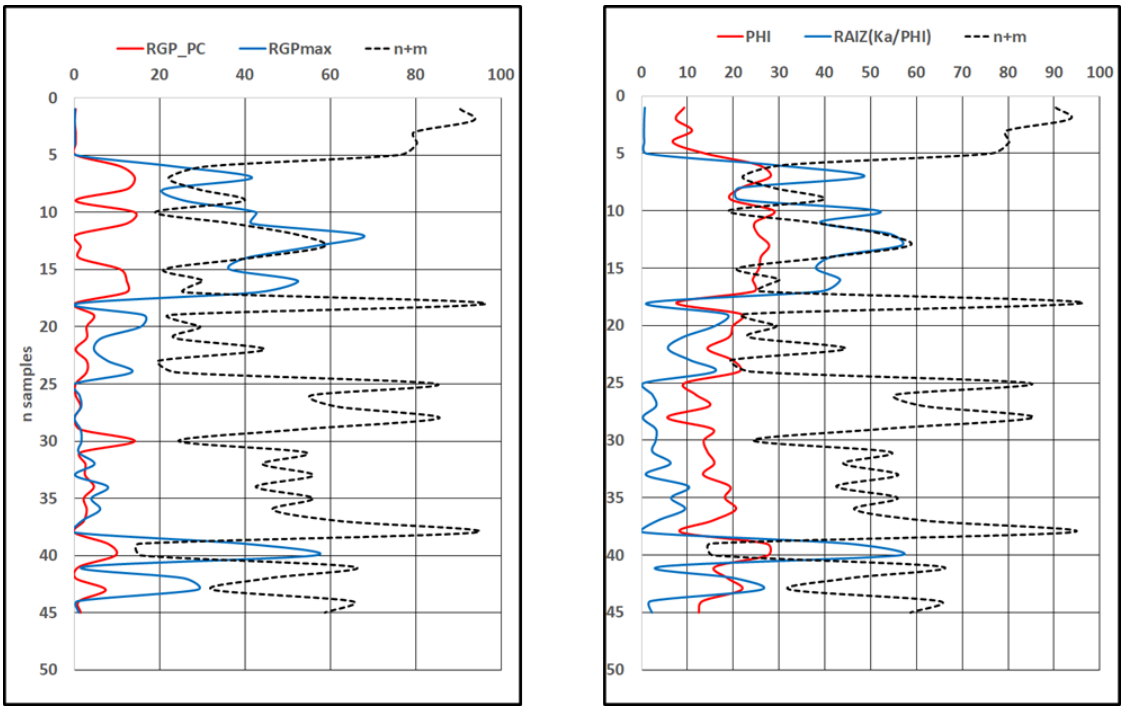

Figure 11.- Comparison of poral sizes, porosity and Ka / PHI root with (nano + microporosity in %).

A good correlation of the Maximum Poral Throat Radius is observed with the poral throat radius from the laboratory with differences in magnitudes, given the plugs heterogeneity present in the interval. There is also correspondence between the sum of nano and microporosity with the porosity and evaluated radius.

The porosity and permeability data to calculate the average porosity and permeability of the composite, was taken from RCAL of plugs that correspond to core 3. For the composite of 3 plugs in which it was made relative permeabilities by dynamic tomography: 5810.7-5810.9 (Plug 15), 5812.4-5812.6 (Plug 18), 5838.5-5838.8 (Plug 38)) which length is 0.54 feet, the average porosity is 0.2278, and the geometric air permeability is 170 md. The dynamic tomography allows calculating petrophysical variables and relative

permeabilities as shown below:

Capillary pressure and gravity effects are neglected

- Kr from CT

$$Kro = \frac{\mu o \; fo}{\vartheta o^{-1}}$$

- fo : fractional flow of oil at the outlet of the plug
- ϑo^{-1} : apparent viscosity at the outlet of the plug

$$Krw = \frac{\mu w \; fw}{\vartheta w^{-1}}$$

- fw : fractional flow of water at the outlet of the plug
- ϑw^{-1} : apparent viscosity at the outlet of the plug

- Porosity from CT

$$\emptyset = \frac{CT1 - CT2}{CTa - CTw}$$

Where.

- $\emptyset$: porosity in each section
- CT1: picture of the CT number of the dry plug
- CT2: Picture of the CT number of plug saturated 100% with water
- CTa: Value of the number on the air
- CTw: Value of the number on the water 100% with water

Figure 12.- Calculation of relative permeabilities and porosity from dynamic tomography.

The process of displacement test in laboratory by dynamic tomography Ortiz [15,16], Colin [6]. is illustrated in Figure 13.

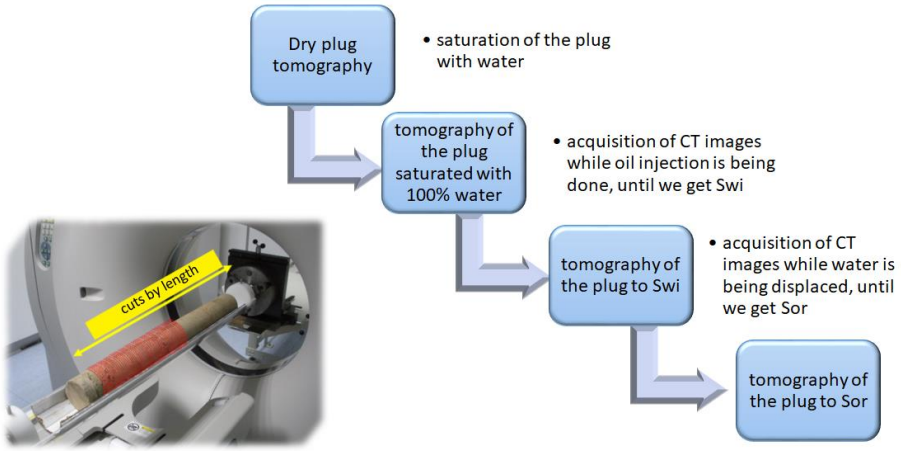

Figure 13.- Dynamic tomography measurement process [14].

To examine the plugs, a comparative study with core is performed. Figure 14 shows the excellent correlation of the estimated porosity of static tomography with the core porosity at depths like those of the dynamic tomography. It is also worth noting the correspondence of PD with the maximum poral throat radius and the characterization of the facies.

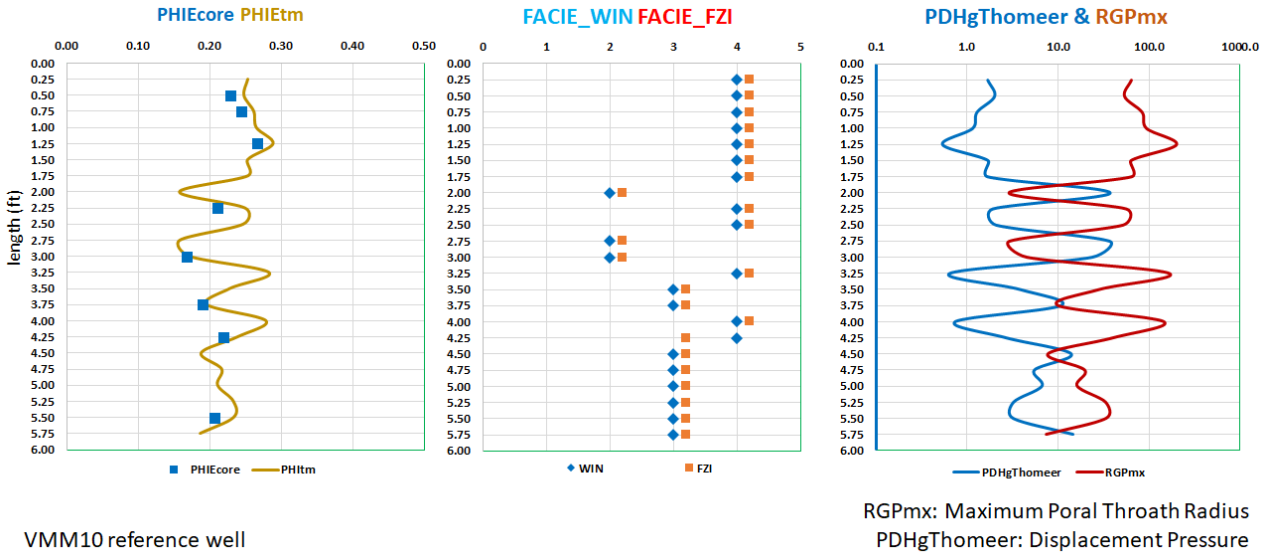

Figure 14.- Comparison of Core Porosities and Static Tomography in the plug.

Using the relative permeability equations of Brooks [11] and the data obtained from PD and RGPmx, the relative permeability solutions were calculated. The results are shown in Figure 15:

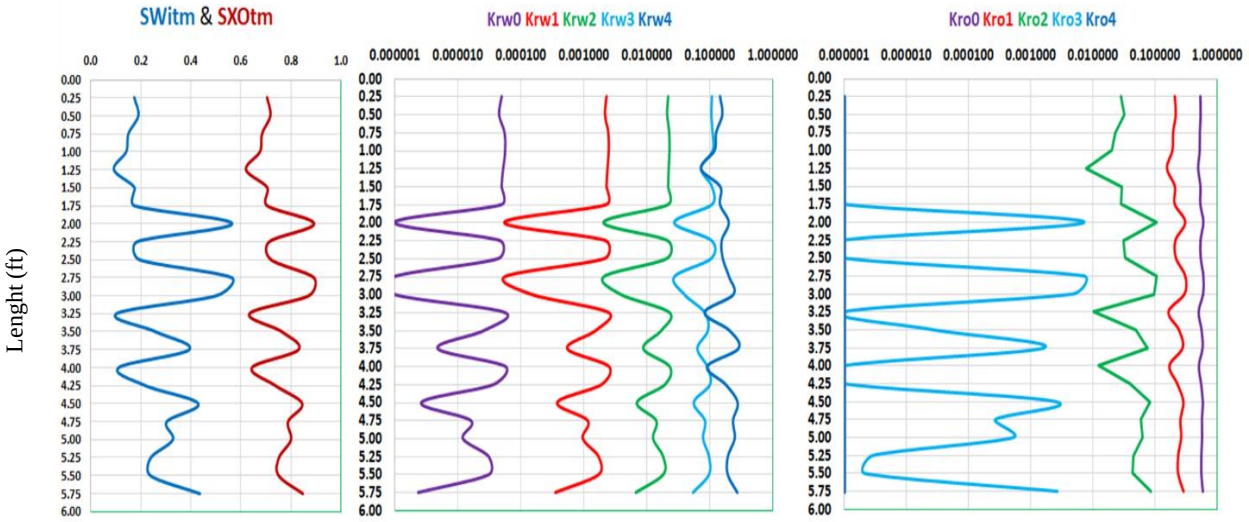

Figure 15.- Comparative of saturations and relative permeabilities of static tomography.

Once the saturation and relative permeabilities data at plug level are normalized, the relative permeabilities graph with respect to water saturation is obtained.

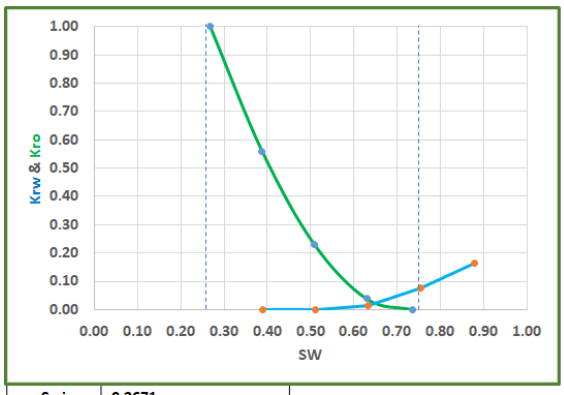

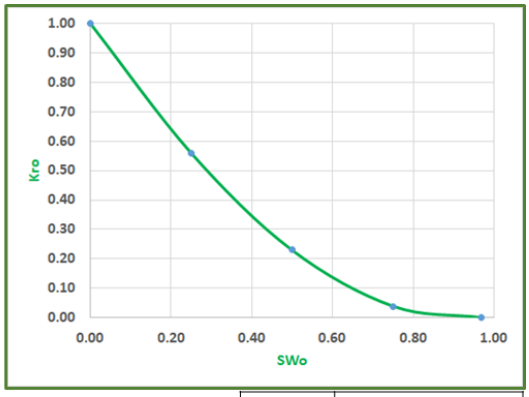

Swi	0,2671	
SXO	0,7511	
SW	SWw	Krw
0,3890	0,167	0,000
0,5110	0,333	0,001
0,6340	0,500	0,013
0,7560	0,667	0,077
0,8780	0,833	0,166

$$Krw = Max(10^{-6}, (SWw^{(2-3*\lambda)/-\lambda}))$$

$$Kro = Max(10^{-6}, Min(1,(1-Swo)^2 * (1-Swo^{(2-\lambda)/-\lambda})))$$

$$SWw = \frac{SW - SWitm}{1 - SWitm} \qquad SWo = \frac{SW - SWitm}{SXOtm - SWitm}$$

Swi	0,2671	
SXO	0,7511	
SW	SWo	Kro
0,2671	0,000	1,000
0,3880	0,250	0,559
0,5090	0,499	0,230
0,6290	0,749	0,039
0,7360	0,969	0,000

Figure 16.- Relative permeabilities from static tomography of the plugs.

Dynamic tomography (DT) relative permeabilities were obtained from a report in the laboratory from 3 added plugs of above-mentioned core 3. For static tomography (ST) relative permeabilities, the 6-foot data were related to the plugs used by the dynamic samples.

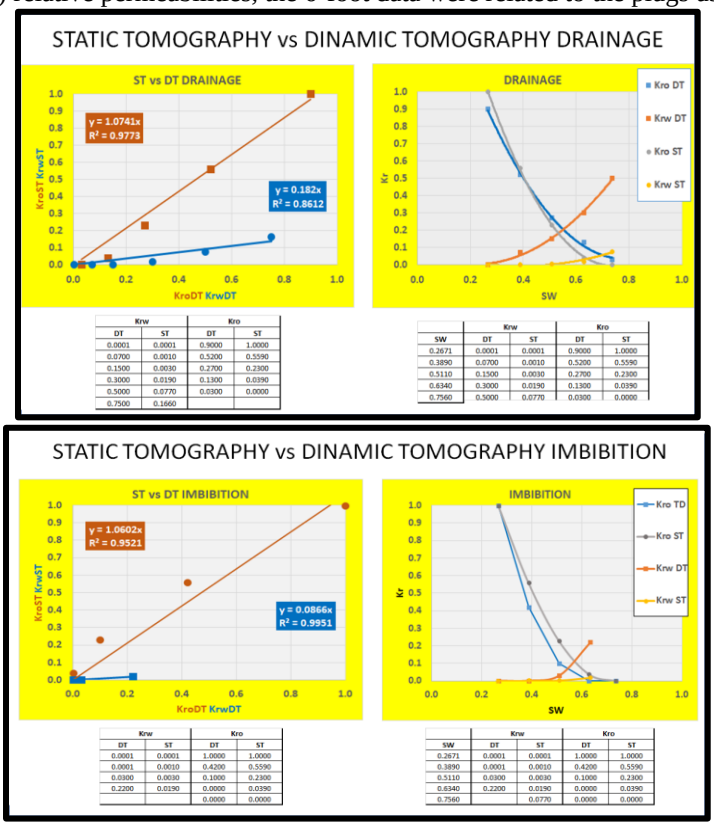

Figure 17.-Relative Permeabilities of Static vs. Dynamic Tomography (Drainage, Imbibition)

It must be noted that the DT measurement is taken directly in the laboratory, while the ST is calculated with the model. Relative permeability results from the ST measurement are indirect. The irreducible water saturation is similar in the two drainage models. The oil relative permeability is similar in DT compared to ST. At 60% water, the Kro in the DT is less than the ST. Water permeability shows differences in both models

Static Tomography

Dynamic Tomography

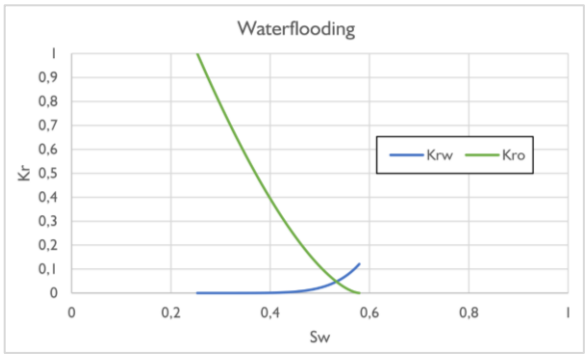

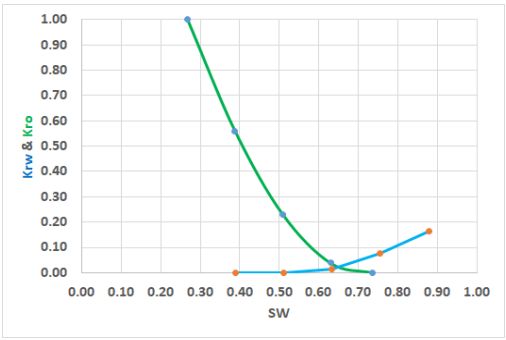

Depth	Porosity Basics	Porosity Petro	Porosity PcHg	Grain Density	Density Skeletal	statistical mode	K KI	K air	Swirr Porous Plate	Swirr centrifuge	Swirr Kr	FACIES
Ft	%	%	%	g/cm3	g/cm3	Microns	mD	mD	%	%	%	
5600.2	19.5	10.74	22.15	2.635	2.618	2.18	12.56	16.25	NR	NR	18.75	Sx
5666.2	18.8	9.81	19.06	2.652	2.678	4.12	17.66	21.55	NR	NR	18.81	Sx
5672.2	22.1	12.00	21.95	2.637	2.539	2.85	87.16	99.41	NR	NR	17.21	Sx
5691.5	16.5	16.72	21.76	2.748	2.620	4.53	17.13	20.88	NR	NR	18.79	Sx
6146.5	17.4	13.79	13.12	2.632	2.662	2.46	62.68	73.62	NR	NR	17.66	Sx
6199.6	21.8	19.37	22.19	2.626	2.676	4.54	109.76	130.12	22.48	38.24	NR	PRESERVED
6210.5	18.7	18.87	20.15	2.653	2.696	1.42	62.46	72.87	NR	NR	17.91	Sx

Depth	Vol. porous	Porosity	KK	K air	Keo-Pre Rest	K porous	Kewf	Swirr	Sor	Np	Krw end point	Cut	Rate Keo	Rate Kewf	Wettability Type	
(ft)	(cm^3)	(%)	(mD)	(mD)	(mD)	Keo-Post (mD)	(mD)	%	%	(%)	(fract)	(fract)	cc/m	cc/m		
5600.2	13.14	19.50	13.00	16.00	5.8	3.4	0.72	18.75	44.89	36.37	0.21	0.43	0.05 - 0.10	1.00 - 0.50	Neutra	Mixta
5666.2	13.01	18.00	18.00	22.00	13.2	2.5	1.67	18.81	42.52	38.67	0.68	0.52	0.05 - 0.10	1.00 - 0.50	Neutra	Mixta
5672.2	15.55	22.10	99.00	87.00	66.3	48.3	8.96	17.21	40.98	41.81	0.19	0.48	0.13 - 0.25	2.00 - 1.00	Neutra	Mixta
5691.5	11.92	16.50	21.00	17.00	11.1	3.6	1.80	18.79	43.38	37.84	0.50	0.58	0.05 - 0.10	2.00 - 1.00	Neutra	Mixta
6146.5	11.83	17.00	63.00	74.00	24.4	6.7	1.32	17.66	40.07	42.27	0.20	0.44	0.125 - 0.06	1.00 - 0.50	Neutra	Mixta
6210.5	12.07	18.70	62.00	73.00	21.4	8.6	2.11	17.91	39.84	42.25	0.25	0.45	0.10 - 0.20	1.00 - 0.50	Neutra	Mixta

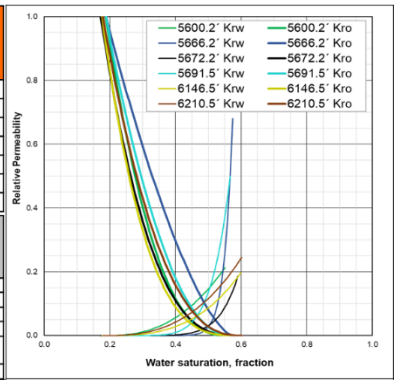

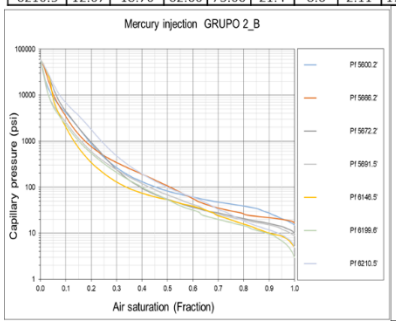

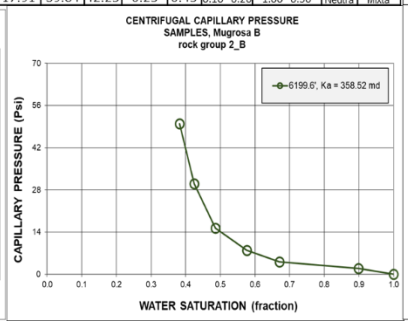

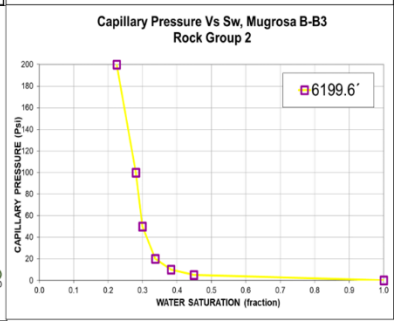

Figure 18.-Relative Permeabilities of Static (A) vs. Dynamic Tomography (B) Vs plugs Unsteady State. Pérez [17]

In case of plugs for the same well Pérez [17], this rock type 2 (Figure 18) presents porosities measured (RCAL) between 16.5% - 22.1%, porosity by MCIP between 13.12% - 22.19%, klinkenberg permeability by basic between 12.56 mD to 109.76 mD. Additionally, it presents Swirr by porous plate of 22.48% and Swirr for relative permeabilities between 17.21% - 18.81%, with a recovery between 36.37% - 42.27% and Neutral-Mixed Wettability. The most similar sample for petrophysical properties when compared plugs Vs the composite DT, is sample 5672.2' with Ka of 99.41 mD, Swirr: 17.21%, Krw (end point): 0.2, Sor: 40.98%, Recovery factor 41.81%, and wettability by Craig's rules to water.

In the case of imbibition, the oil relative permeability in DT is closed but lower than in ST. The water relative permeability in the imbibition case shows greater differences than in the drainage case. In terms of water cut, there would be an earlier water cut from the DT curves compared with ST. While porosity and permeability are properties of the porous medium, relative permeability is not. Even specifying the porous medium and the fluids, the relative permeability curves in the reservoir depend strongly on the production mechanisms (capillary, gravitational and viscous forces), while at laboratory level, viscous forces predominate, which can favor the invasion of larger poral radius throats Crotti [17] generating a wetting behavior similar to oil wet rock, which favors an earlier high water cut.

It is considered that the proposed methodology leads to good results of the different petrophysical variables as porosity and irreducible water saturation. It is essential to pursue the investigation to establish adjustments and procedures seeking an effective integration of the static tests with the dynamic tests, mainly in the relative permeability calculation.

Conclusions

1. The relative permeability prediction model proposed in this paper uses data from static tomography as the start of the workflow, and estimates capillary pressure, pore geometry, and its distribution with respect to saturation from effective porosity and permeability considering tomography-logs-core scaling.

2. Given the different resolutions of the available data, mechanisms were established to facilitate their comparison. Scaling (633 final data Vs 74302 Original data) was performed using logs, cores and static tomography data as initial comparison to verify that the scaling was adequate and then at the level of core plugs with static tomography data to corroborate results. The estimated average values (633 data) were estimated from the quality control of the static tomography data using filters to eliminate empty data or with erroneous response from the tomograph due to core termination.

3. In the proposed model, the Amaefule equation was modified, which allows the calculation of SWi since the porosity is known by core static tomography (full diameter size) and the permeability by plugs (RCAL).

4. The scaling profile of the porosity by static tomography correlates quite well and the differences in porosity between plug (RCAL) and core, are explained by the reservoir heterogeneity.

5. In the proposed model, an excellent correlation is observed between the displacement pressure (PD), the irreducible water saturation SWi, and the calculated flow units. A similar case occurs with the correlation between relative permeabilities calculated from static tomography and porosities from static tomography, logs, and cores. Also noteworthy is the excellent correlation of the estimated porosity of the static tomography with the porosity of plugs at depths similar to the dynamic tomography. Therefore, the use of a density of 2.65 gr / cc is adequate as sandstone and it is verified with PEF values <2.5.

6. From the analysis of the results obtained with the proposed model, it can be concluded that there is a direct correspondence between the pore throat radius for PC (RGP_PC), the radius of pore throat for maximum (RGPmax) and porosities, while there is an inverse correspondence of the radius and porosities evaluated with the sum of the microporous plus nano volumes in the samples.

7. The samples used in the capillary pressure measurements (PC) in the laboratory showed high heterogeneity in the core interval analyzed, highlighting the abundant presence of nano poral throat radius and microporosity.

8. Relative permeabilities obtained by dynamic tomography are considered reliable and representative as this is a direct measurement, when comparing the results with previous unsteady state permeability tests performed on rock Type 2 plugs from the same well.

9. Differences were observed when comparing the relative permeabilities calculated, by integration of static and dynamic tomography. Differences among parameters such as Sor and Krw with the equivalents reported from the lab dynamic tomography using plugs are observed.

Acknowledgments

The Colombian Oil Company (ECOPETROL ICP) are to be thanked for providing the data and supporting this research, and the School of Petroleum Engineering of the Industrial University of Santander UIS, for the support to continue this work and corroborate the methods used.

REFERENCES

[1] Tarazona, A.S., Bejarano, A., Olaya, H., & Perez, E.R. (2020). "Metodología de modelamiento de permeabilidades relativas combinando el método de Thoomer modificado con datos de tomografía, núcleos y registros." In *61st SPWLA Annual Student Presentation Contest.* Society of Petrophysicists and Well Log Analysts. wq

[2] Zhao, H., Ning, Z., Zhao, T., Zhang, R., & Wang, Q. (2016). "Effects of mineralogy on petrophysical properties and permeability estimation of the Upper Triassic Yanchang tight oil sandstones in Ordos Basin", *Northern China. Fuel, 186,* 328-338. https://doi.org/10.1016/j.fuel.2016.08.096

[3] Ortiz-Meneses, A. F., Chaves-Plata, J. M., Herrera-Otero, E.H., & Santos-Santos, N. (2015). "Caracterización estática de rocas por medio de tomografía computarizada de Rayos-X TAC". *Fuentes, el reventón energético, 13*(1), 57-63. https://doi.org/10.18273/revfue.v13n1-2015005

[4] Amaefule, J. O., Altunbay, M., Tiab, D., Kersey, D. G., & Keelan, D. K. (1993, January). "Enhanced reservoir description: using core and log data to identify hydraulic (flow) units and predict permeability in uncored intervals/wells". In *SPE annual technical conference and exhibition*. Society of Petroleum Engineers. SPE 26436. https://doi.org/10.2118/26436-MS

[5] Fu, D., Belhaj, H., & Bera, A. (2018). "Modeling and simulation of transition zones in tight carbonate reservoirs by incorporation of improved rock typing and hysteresis models". *Journal of Petroleum Exploration and Production Technology, 8*(4), 1051-1068. https://doi.org/10.1007/s13202-018-0463-2

[6] Colin, K.L.; Terán, A.E. (2019). "Determinación de curvas de permeabilidad relativa asistida por tomografía de rayos-X (Tesis)", Instituto Politécnico Nacional, Ciudad de México. Available electronically from https://tesis.ipn.mx/bitstream/handle/123456789/26993/Determinaci%C3%B3n%20de%20curvas%20de%20permeabilidad%20relativa%20asistida%20por%20tomograf%C3%ADa%20de%20Rayos-X.pdf?sequence=1&isAllowed=y

[7] Thomeer, J. H. M. (1960). "Introduction of a pore geometrical factor defined by the capillary pressure curve". *Journal of Petroleum Technology, 12*(03), 73-77. https://doi.org/10.2118/1324-G

[8] Wu, Tao (2004). "Permeability prediction and drainage capillary pressure simulation in sandstone reservoirs". Doctoral dissertation, *Texas A&M University. Texas A&M University*. Available electronically from http://hdl .handle .net /1969 .1 /1496.

[9] Clerke, E. A., Mueller III, H. W., Phillips, E. C., Eyvazzadeh, R. Y., Jones, D. H., Ramamoorthy, R., & Srivastava, A. (2008). "Application of Thomeer Hyperbolas to decode the pore systems, facies and reservoir properties of the Upper Jurassic Arab D Limestone, Ghawar field, Saudi Arabia: A "Rosetta Stone" approach". *GeoArabia, 13*(4), 113-160.

[10] Harris, T. G., Luffel, D. L., & Hawkins, J. M. (1997). *U.S. Patent* **No. 5,621,169**. "Method for determining hydrocarbon/water contact level for oil and gas wells. Washington", DC: U.S. *Patent and Trademark Office*.

[11] Brooks, R. H., & Corey, A. T. (1964). "Hydraulic properties of porous media" (Doctoral dissertation). *Colorado State University*. Available electronically from https://mountainscholar.org/bitstream/handle/10217/61288/HydrologyPapers_n3.pdf?se

[12] Leverett, M.C. "Capillary Behavior in Porous Solids." Trans. 142 (1941): 152–169. doi: https://doi.org/10.2118/941152-G

[13] Kolodzie, Stanley. "Analysis Of Pore Throat Size And Use Of The Waxman-Smits Equation To Determine OOIP In Spindle Field, Colorado." Paper presented at the *SPE Annual Technical Conference and Exhibition*, Dallas, Texas, September 1980. doi: https://doi.org/10.2118/9382-MS

[14] Bejarano W. Aristobulo, "Reservoir Characterization Lectures", UIS 2015, Notes about Amaefule modified. Trabajo interno UIS.

[15] Ortiz-Meneses, A. F., Herrera-Otero, E.H., & Santos-Santos, N. (2017). "Estimación de saturaciones in-situ durante experimentos de inyección de fluidos usando tomografía computarizada de rayos X". *Fuentes, el reventón energético, 15*(2), 107-116. https://doi.org/10.18273/revfue.v15n2-2017009

[16] Ortiz-Meneses, A. F., Carrillo-M, L.F, Herrera-Otero, E.H, & Santos-Santos, N. (2019, January). "Experimental Estimation of Relative Permeabilities Through Computed Tomography". In *SPWLA 60th Annual Logging Symposium*. Society of Petrophysicists and Well-Log Analysts. https://doi.org/10.30632/T60ALS-2019_NNNN

[17] Crotti, M. (2013). La Acción de las Fuerzas Capilares y Gravitatorias sobre la Curva de Flujo Fraccional. Nota Técnica 01-2013. Available electronically from http://www.inlab.com.ar/2013_01_Efect_Cap_Grav_sobre_fw.pdf

[18] Perez, E.R., Ayerim, O., Carreño, A., & otros (2019). Informe integrado de análisis de laboratorio de petrofísica, mineralogía y sedimentología de la Formación Mugrosa (zonas B y C), en el pozo Llanito P-38. Informe técnico de *Ecopetrol.*

NOMENCLATURE

CT= Computed tomography (voxel)
DT= Dynamic Tomography
Fg= porous geometric factor
FZI_H= Hydraulic unit of Flow zone Indicator
FZI_VALUE= Value amounts the hydraulic unit of the Flow Zone Indicator
FZI= Flow zone indicator
ICI= information quality index
IPM= Mercury Injection Porosimeter
J (SW)= J Leverett (fraction)

K= Permeability (md)
Ka= air Permeability
Kro= Oil relative permeability
Kro= Permeability relative to oil
Krw= Permeability relative to water
Krw= Permeability relative to water
MCIP= Mercury injection capillary pressure (percentage)
MICP= Mercury Injection Capillary Pressure
NR= non register
Øe= effective porosities(fraction)
Øt= total porosities (fraction)
PC= Capillary Pressure (psi)
PCHgmx= Maximum Mercury-Air Capillary Pressure (psi)
PCowmx= Maximum Oil-Water Capillary Pressure (psi)
PD= Displacement pressure (psi)
PDHGThomeer= Mercury Displacement Pressure of Thomeer
PEF= Photoelectric potential
PHI= Porosity (fraction)
PHIDtm= tomography dynamic porosity (fraction)
PHIEcore= Porosity Effective core
PHIElog= Porosity Effective log
PHIEtm= Porosity Effective tomography
PHITlog= Porosity Total log
Plug= one core plug
PTR= poral throat radius
R35= Winland Poral Throat Radius (microns)
RCAL= Routine core Analysis.
RGP_PC= Poral throat Radius Capillary Pressure
RGPmx= Maximum Poral Throat Radius
RHOB= Density of the rock-fluid system
rmh= average radius of the hydraulic unit
RQI= reservoir quality index
SEM= Scanning electron microscopy
SOR= residual oil saturation (fraction)
ST= Static Tomography
SW= water saturation (fraction)
SWi= Irreducible water saturation (fraction)
SWo= Fraction of mobile water with SOR to SW
SWw= Fraction of moving water to SW
SXO= 1-SOR (fraction)
WIN_H= Hydraulic unit of Winland
WIN_VALUE= Value amounts the hydraulic unit of Winland
XRD= X-ray diffraction
Zeff= Effective atomic number
λ= Slope of log (PC) vs log (SW)